Effect of heat treatments on Inconel 625 fabricated by wire and arc additive manufacturing: an in situ synchrotron X-ray diffraction analysis

Tiago A. Rodrigues, Francisco Werley Cipriano Farias, Julian A. Avila, Emad Maawad, Norbert Schell, Telmo G. Santos & J. P. Oliveira

I·M3
Institute of Materials, Minerals & Mining

Taylor & Francis
Taylor & Francis Group

Effect of heat treatments on Inconel 625 fabricated by wire and arc additive manufacturing: an in situ synchrotron X-ray diffraction analysis

Tiago A. Rodrigues[a], Francisco Werley Cipriano Farias[a], Julian A. Avila[b], Emad Maawad[c], Norbert Schell[c], Telmo G. Santos[a] and J. P. Oliveira [a,d]

[a]UNIDEMI, Department of Mechanical and Industrial Engineering, NOVA School of Science and Technology, Universidade NOVA de Lisboa Caparica, Portugal; [b]Department of Strength of Materials and Structural Engineering, Barcelona School of Engineering (ETSEIB), Universitat Politècnica de Catalunya, Barcelona, Spain; [c]Helmholtz-Zentrum Hereon, Institute of Materials Physics, Geesthacht, Germany; [d]CENIMAT/I3N, Department of Materials Science, NOVA School of Science and Technology, Universidade NOVA de Lisboa, Caparica, Portugal

ABSTRACT

The effect of heat treatments on wire and arc additively manufactured Inconel 625 parts was investigated using in situ synchrotron X-ray diffraction and hardness testing. As-built samples revealed the presence of a γ-matrix with precipitation of γ', γ'' and MC carbides. When heat treated at 750°C for 4 h, γ'' phase precipitated increasing the hardness by 5%. In situ X-ray observations revealed that heat treating at 870°C for 1 h resulted in δ-phase precipitation. Two different second-stage temperatures were tested (1050°C and 1150°C), which dissolved the δ-phase while MC carbides formed upon cooling. The second stage at 1150°C had a higher deleterious effect than the one performed at 1050°C due to extensive grain growth.

Introduction

Nickel-based superalloys are the second most popular material studied by the additive manufacturing (AM) community after titanium alloys, which is mainly due to their high fabrication cost using traditional methods and outstanding performance at high temperatures. Inconel 625 is a solid solution strengthened Ni-based alloy initially developed as a replacement for stainless steel 316 in steam power plants. However, it is commonly used in marine, nuclear and chemical processing applications where moderate strength and creep resistance are required at elevated temperatures (up to 800°C) [1].

The microstructure of Inconel 625 after welding or fusion-based additive manufacturing cannot be directly compared with its wrought counterparts, as the enrichment of Nb in the interdendritic region during solidification favours the formation of MC (M: Nb, Ti) carbides and Laves phase (A$_2$B, A: Ni, Cr, and Fe; B: Nb, Mo, Ti; D0$_{24}$; hexagonal; P6$_3$/mmc) by eutectic reactions [2]. Fusion-based welding of Inconel 625 is overall well established in the literature [3–5], and this can be used to guide process parameters developed in fusion-based additive manufacturing of this material. Precipitation of blocky M$_6$C (M: Si, Ni, Cr) and M$_{23}$C$_6$ (M: Cr) carbides can also occur in the

760–980°C temperature range. Segregation and precipitation of the Laves phase, which possesses a low melting point, increase the solidification range temperature and reduce the alloy weldability or printability (due to hot cracking – liquation and solidification) [6]. This alloy is a solid solution strengthened. However, the precipitation of intermetallic phases, such as γ' (Ni$_3$Al, Ti; L$_{12}$; cubic, Pm3$^-$m) and metastable γ'' (Ni$_3$Nb; D0$_{22}$; tetragonal; I4/mmm) can occur during thermal cycling induced by heat treatments and/or AM processes. Moreover, the precipitation of undesirable δ-phase (Ni$_3$Nb; D0$_a$; orthorhombic; Pmmn) can reduce the material ductility and toughness. This phase can directly precipitate from γ at ageing temperatures below 750°C or replace the γ'' phase when exposed to higher temperatures (750 < T < 950°C) [7,8]. Even though the δ-phase is thermodynamically more stable than γ'', the slow precipitation kinetics of the δ-phase allows the γ'' phase to precipitate first [9].

Post-process heat treatments performed in solid-solution strengthened alloys are conducted for several reasons, including dissolving undesirable secondary phases, homogenising and relieving residual stresses. Since the effect of the heat treatments largely depends on the initial condition of the superalloy microstructure, the already commonly studied heat treatments for

Table 1. Chemical composition of the ER NiCrMo-3 wire electrode (wt-%).

Ni	C	Si	Mn	Al	Co	Cr	Cu	Fe	Mo	Nb	Ti
Bal.	0.1	0.5	0.5	0.4	1	21.5	0.5	5	9	3.5	0.4

Inconel 625 processed by traditional means (ex: casting) may have a different effect on Inconel 625 parts fabricated by AM technologies. Recommended stress-relief heat treatments for Inconel 625 are done in the 700–900°C temperature range [2]. However, in AM parts, at a temperature of 800 °C, the δ-phase precipitates in just 4 h, and when the ageing temperature is raised to 870°C, the kinetics of δ-phase precipitation is increased, as 1 h is enough to form a significant volume fraction (between 5% and –10%) [10]. An 8 h heat treatment at different temperatures was performed by Cortial et al. [11] on welded Inconel 625. In the temperature range of 650–750°C, the improved mechanical strength and decreased ductility were linked to the precipitation of the γ'' phase. Between 750°C and 950°C, the γ'' phase dissolved, and the orthorhombic intermetallic δ phase formed deteriorating the hardness, yield strength, ultimate tensile strength, ductility and impact strength. Above 850°C, M_6C carbides formed along the grain boundaries. At 1000°C, the ductility and impact strength are partially restored due to the dissolution of the δ-phase, and the amount of M_6C grain boundary carbides increased slightly. This occurred since the increased size of the grains is no longer blocked by the existence and size of the precipitates.

Xu et al. [12] studied the effect of heat treatments on Inconel 625 parts fabricated by Wire and Arc Additive Manufacturing (WAAM) and found that heat treatment of 980°C for 1 h dissolved a large amount of the Laves phase and led to the precipitation of the δ phase. The heat treatment at 1080°C for 1 h resulted in the complete dissolution of the Laves phase, and the mechanical properties were severely diminished due to the excessive grain growth. Grain growth occurs due to the dissolution of the δ phase, which will no longer pin the grain boundaries during the heat treatment.

Typically, the properties of as-built AMed Inconel 625 are better than those after heat treatment. However, post-process heat treatments can still provide improved corrosion resistance and reduce residual stresses that originate from the multiple heating and cooling cycles experienced by the material during fusion-based AM. In these cases, finding appropriate heat treatments to prevent embrittlement of Inconel 625 parts is of interest given the relevance of this material in multiple key industries. This work assesses by in situ X-ray diffraction measurements the effect of different heat treatments on the microstructure evolution of Inconel 625 parts fabricated by WAAM.

Experimental procedure

In this study, a 55-layer WAAM single wall with 110 mm length was fabricated using an in-house custom-made WAAM apparatus, which included a customised gas metal arc welding (GMAW) torch. The wire feedstock used in this work was a commercial Inconel 625 (ER NiCrMo-3) with 1 mm in diameter, the chemical composition is given in Table 1. A wire feed speed of 4 m min^{-1}, a travel speed of 250 mm min^{-1}, a voltage of 19 V and a current of 73 A were used, as the molten pool was protected with 99.99% argon. A zig-zag deposition strategy with 90 s of idle time between each torch stop/start was used.

Four different post-WAAM heat treatments were performed in situ at the High Energy Materials Science beamline at PETRA III, DESY (Hamburg, Germany) with a beam energy of 100 keV (0.1234 Å): (i) 750°C for 4 h, followed by forced gas cooling (Ar); (ii) 870°C during 1 h followed by another 1 h at 1050°C, followed by forced gas cooling (Ar); (iii) 870°C for 1 h plus another 1 h at 1150 °C, followed by forced gas cooling (Ar) and finally (iv) 1200°C for 30 min, followed by forced gas cooling (Ar). The heating and cooling rates were set to 10°C s^{-1}. A 2D Perkin Elmer detector with a pixel size of 200 µm was used to capture the Debye-Scherrer diffraction rings. Fit2D software was used to integrate the rings along the full azimuthal angle (ϕ) to obtain conventional (intensity vs. d-spacing) diffractograms. The beam size was 1×1 mm, and the sample-to-detector distance was determined to be 1517 mm. The sample-to-detector distance and the detector tilt were calibrated using LaB_6 calibrant powder. A beam exposure time of 5 s was used, and diffraction images were taken continuously during the whole heat treatment schedule.

Hardness measurements were performed using a Mitutoyo HM-112 Hardness Testing Machine, under a load of 0.5 N for 10 s. A matrix of 5×5 mm was made with a distance between indentations of 1 mm. A Leica 5000 M inverted optical microscope and a SU3800 Hitachi scanning electron microscope were used to examine the samples, after being electro-etched with a solution of 10 g CrO_3 and 100 mL H_2O. A 5 V DC power supply was used and the chemical attack lasted 15 s.

ThermoCalc was used with the TCNI8 thermodynamic database to address the phases that would form during solidification and with the experienced thermal cycles. The Scheil-Gulliver model was used, and
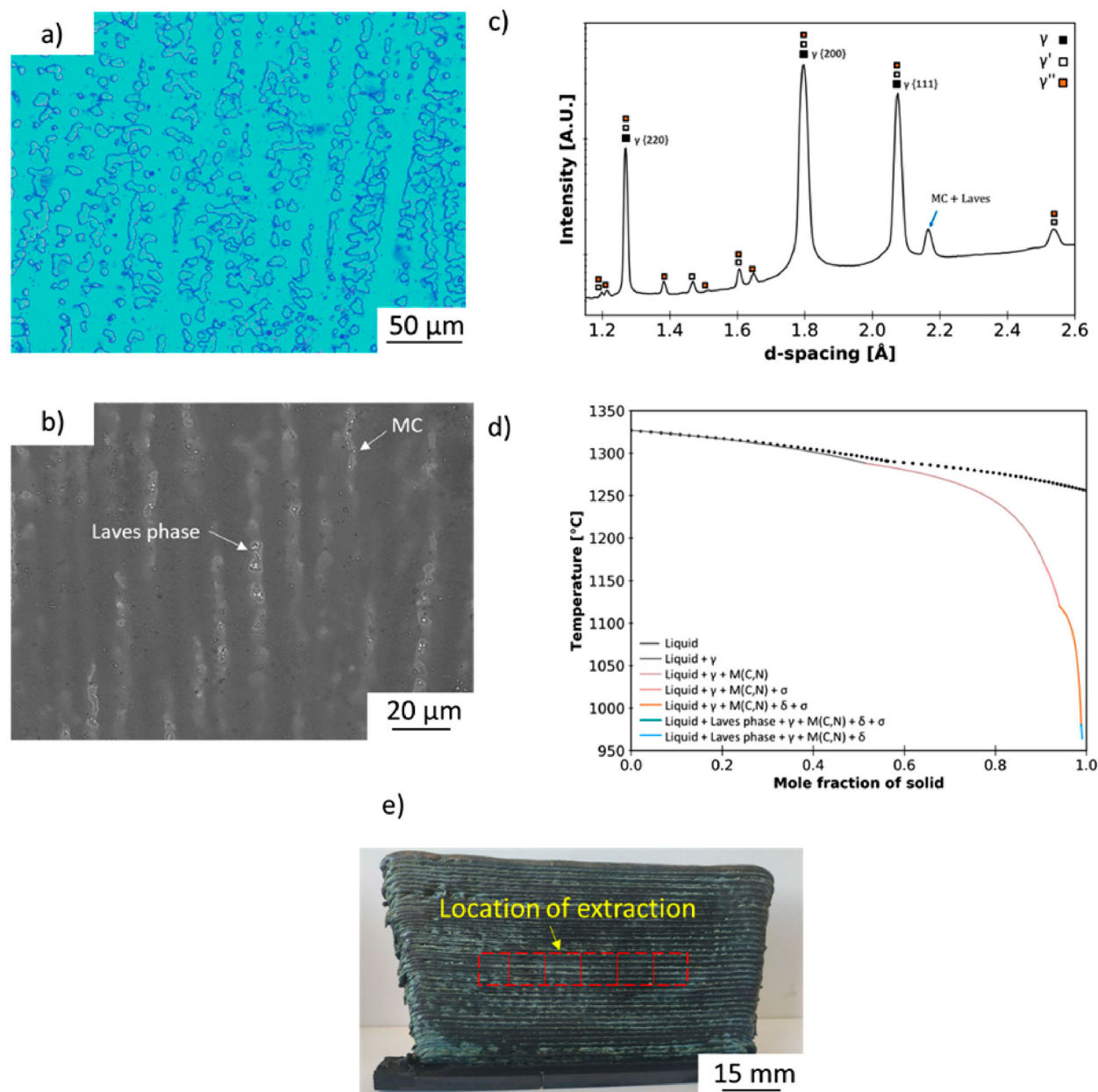
Figure 1. (a) Optical microscope observation of as-built Inconel 625; (b) SEM image of the inside of the γ-dendrites; (c) synchrotron X-ray diffraction pattern of the Inconel 625 as-built sample; (d) Scheil-Gulliver calculations and (e) indication of the region where the specimens were removed from the Inconel 625 part.

it assumes equilibrium at the solid/liquid interface, complete diffusion in the liquid, negligible diffusion in the solid and negligible dendrite tip undercooling [13].

Results and discussion

The microstructure of the as-built sample is depicted in Figure 1(a) and presents columnar dendrites aligned with the build-up direction. Figure 1(b) depicts an SEM micrograph of the as-built microstructure, in which precipitates are visible inside the γ-dendrites resembling the Laves phase morphology and MC-type carbides. These carbides can play a role in pinning the migration of grain boundaries, increasing the alloy strength [14]. A representative synchrotron X-ray diffraction pattern of the as-built sample is detailed

in Figure 1(c). It is shown that the material is mainly composed of an γ-matrix with γ', γ'', Laves phase and MC-type carbides. A strong growth texture due to preferred solidification along the $\langle 100 \rangle$ crystallographic direction resulted in a high 200_γ peak intensity. Based on the Scheil–Gulliver calculations (refer to Figure 1(d)), this superalloy solidification sequence starts with the Liquid $\rightarrow \gamma$ reaction, followed by MC precipitation via eutectic reaction (Liquid $\rightarrow \gamma + $MC). The rejection of alloying elements, such as Nb and Mo, to the interdendritic regions, favours the enrichment of the γ-dendrites, favouring the precipitation of eutectic products. Besides Laves, the Scheil–Gulliver calculations predicted precipitation of σ and δ, which were not observed in the synchrotron X-ray diffraction patterns.
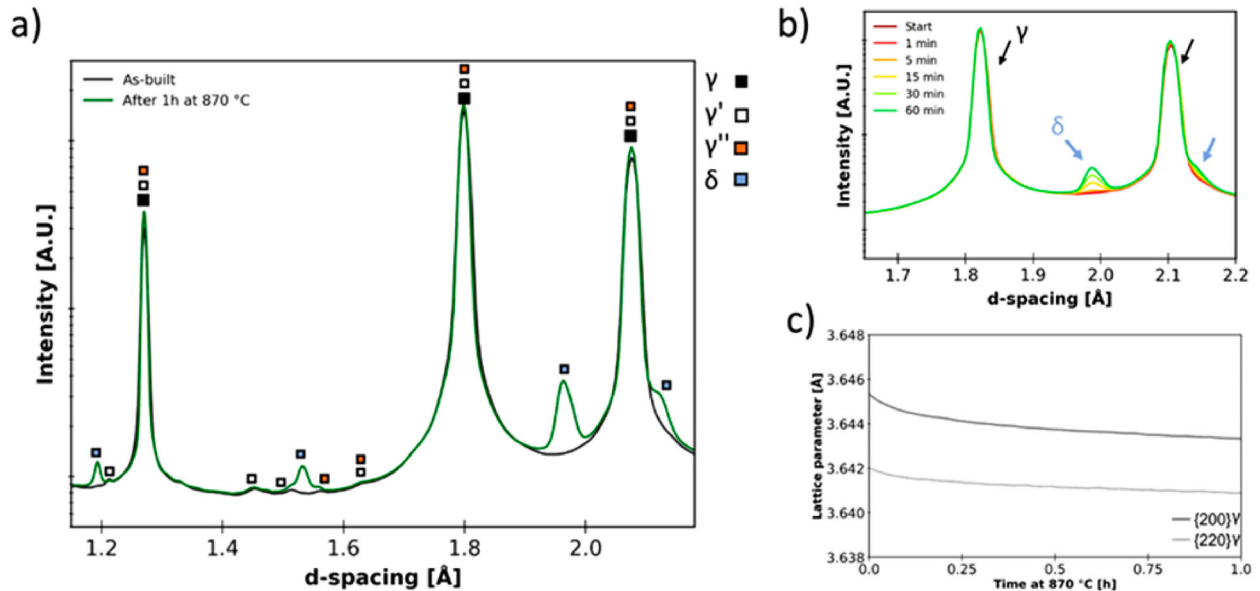
Figure 2. (a) Synchrotron X-ray diffraction patterns of the Inconel 625 WAAM sample after 1 h at 870°C; (b) Detail of the δ-phase precipitation at 1, 5, 15, 30 and 60 min during isothermal holding and (c) lattice parameter evolution of γ 200 and γ 220 peaks.

The first annealing temperature of 870°C was intended to relieve the stresses formed during WAAM, which can be up to 525 MPa [15]. This temperature is the industry-recommended stress relief temperature for Inconel 625 parts. However, 1 h at 870°C was responsible for the precipitation of the undesired δ-phase during isothermal holding (refer to Figure 2(a)). Xing et al. [16] studied the transformation of γ'' to δ, concluding that δ forms in the stacking faults of the close-packed plane of the γ'' phase by shear mode, which resembles the bainite transformation in steels.

As the time-resolved X-ray diffraction patterns results show (refer to Figure 2(b)), the δ-phase rapidly starts to form, within less than 5 min of heat treatment and 1 h was not sufficient to fully dissolve the γ'' phase. Since the presence of δ is detrimental to the material mechanical properties, a second-stage heat treatment is necessary to dissolve it. The lattice parameter evolution of the γ 200 and γ 220 peaks is presented in Figure 2(c). As δ forms, it removes Nb from the matrix, thus resulting in a decrease of the lattice parameter in the γ-phase.

The homogenisation heat treatments at 1050°C and 1150°C were designed to dissolve other segregation-induced phases in the as-built samples into the matrix while minimising grain growth. The second step of both heat treatments (1050°C and 1150°C) was responsible for the dissolution of the previously formed δ-phase. During heating (refer to Figure 3(a)), the δ-phase diffraction peaks become untraceable at approximately 1000°C. Moreover, during cooling from 1150°C, MC-type carbides are formed and stabilised at room temperature (Figure 3(b)). In the literature, some authors have suggested that the δ-phase can be formed at temperatures as high as 1050°C [17], which was not verified in the current work, as the heat treatment performed at 1050°C fully dissolved the δ phase. This can be related to composition changes induced by the non-equilibrium solidification conditions typical of WAAM.

The presented results do not follow those previously presented in the literature, which showed that M_6C precipitates form during stress relief heat treatment (870°C for 1 h) and that the homogenisation heat treatment (1150°C for 1 h) promoted Laves phase precipitation and grain growth without dissolving the M_6C carbides [18]. Again, the existence of a highly segregated microstructure (compared to wrought parts) can justify this mismatch, as also observed in 316L stainless steel fabricated by WAAM [19].

The heat treatment performed at 750°C for 4 h showed that γ'' (Ni$_3$Nb) phase has precipitated and becomes noticeable by a peak broadening of the main γ peaks, as seen in Figure 4(a). The X-ray diffraction patterns of the sample heat treated at 1200°C for 30 min confirmed that the carbides, γ' and γ'' phases that formed during fabrication remain unchanged (Figure 4(b)).

Hardness measurements (Figure 5) showed that the selected heat treatments on Inconel 625 WAAM parts can have a significant impact on the final material hardness. The as-built sample had an average hardness of 225 HV. With the heat treatment at 750°C, the γ'' precipitation increased hardness by 11 HV (an increase of $\approx 5\%$). Between the heat treatments that started with the stress relief heat treatment (870°C for 1 h) followed by annealing, the sample annealed at 1150°C resulted in a decrease of the hardness of 21 HV (a decrease of $\approx 10\%$), while the one performed at 1050°C experienced only a marginal decrease of 2 HV. This difference is related to a plausible extensive grain growth effect experienced by the sample heat treated at 1150°C since the phases present in both samples afterward were the
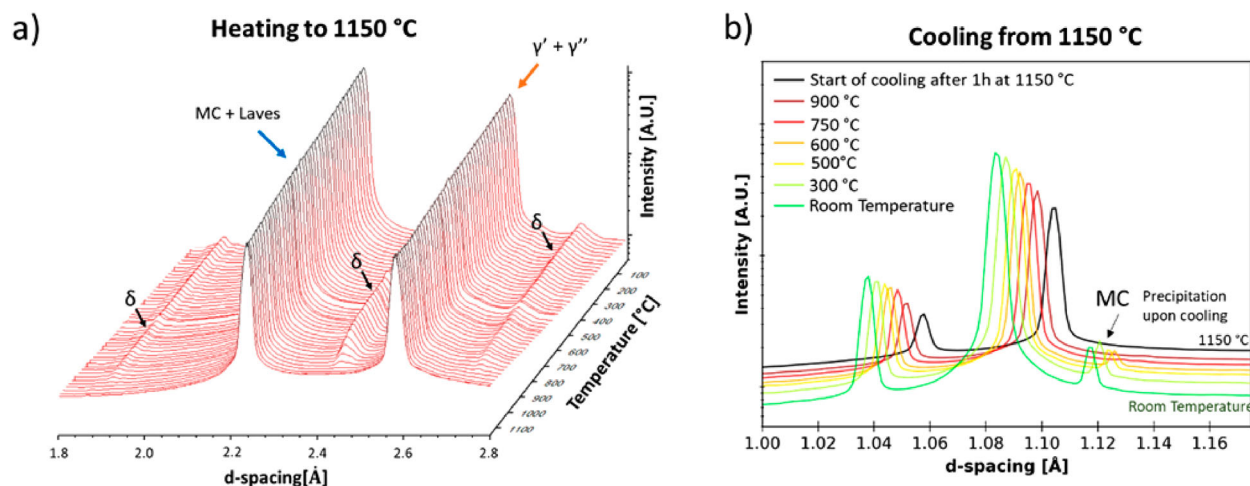
Figure 3. Secondary precipitates (δ) formation during heating up to 1150°C and (b) MC-type carbides formation during cooling from 1150°C down to room temperature.
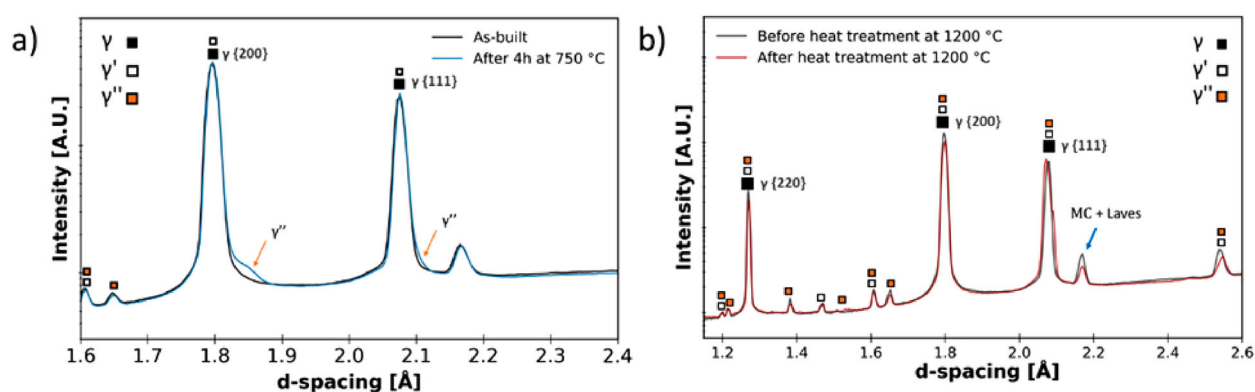
Figure 4. Synchrotron X-ray diffraction results after heat treatment for (a) 4 h at 750°C and (b) 30 min at 1200°C.
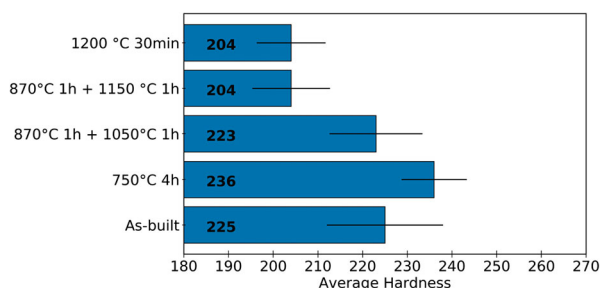
Figure 5. Hardness measurements were taken by mapping an area of 5 × 5 mm with a step size of 250 μm.

same. In conclusion, regarding the mechanical properties, there was no significant difference between the second step heat treatment performed at 1150 °C at 1 h, with the heat treatment performed at 1200°C for 30 min.

Conclusions

In this work, the effect of post-process WAAM heat treatments applied on Inconel 625 parts was evaluated. By combining hardness measurements with in situ X-ray diffraction measurements, the following was concluded:

- The as-built samples presented a γ matrix with γ',γ'', MC carbides and Laves phase as secondary phases;
- After the stress relief at 870°C, synchrotron X-ray diffraction showed the appearance of the δ phase, and as it forms, it removes Nb from the matrix, thus decreasing the lattice parameter of the γ phase;
- Both annealings performed at 1050°C and 1150°C for 1 h fully dissolved the δ phase. However, the combination of time and temperature was not enough to dissolve both carbides and Laves that were already present in the as-built condition. The annealing at 1050 °C did not affect the hardness measurements, but at 1150°C, hardness decreased by approximately 10%;
- The heat treatment performed at 750°C for 4 h showed γ'' (Ni$_3$Nb) precipitation and, therefore, an increase of hardness from 225 HV to 236 HV.

ORCID

J. P. Oliveira ![ORCID icon] http://orcid.org/0000-0001-6906-1870

References

[1] Shankar V, Bhanu Sankara Rao K, Mannan S. Microstructure and mechanical properties of Inconel 625 superalloy. J Nucl Mater. 2001;288:222–232. doi:10.1016/S0022-3115(00)00723-6.

[2] DuPont JN, Lippold JC, Kiser SD. Welding metallurgy and weldability of nickel-base alloys. Hoboken (NJ): John Wiley & Sons, Inc.; 2009. doi:10.1002/9780470500262.

[3] Ruiz-Vela JI, Montes-Rodríguez JJ, Rodríguez-Morales E, et al. Effect of cold metal transfer and gas tungsten arc welding processes on the metallurgical and mechanical properties of Inconel® 625 weldings. Weld World. 2019;63:459–479. doi:10.1007/s40194-018-0661-z.

[4] Azari M, Rasti E, Dehkordi MHR, et al. Investigation of temperature distribution and melt pool microstructure in laser fusion welding of Inconel 625 superalloy. J Laser Appl. 2021;33:022015. doi:10.2351/7.0000376.

[5] Won Han J. Investigation of the weld properties of Inconel 625 based on Nb content. Int J Electrochem Sci. 2018: 2829–2841. doi:10.20964/2018.03.01.

[6] DuPont JN, Robino CV, Michael JR, et al. Solidification of Nb-bearing superalloys: part I. Reaction sequences. Metall Mater Trans A Phys Metall Mater Sci. 1998;29:2785–2796. doi:10.1007/s11661-998-0319-3.

[7] Sundararaman M, Mukhopadhyay P, Banerjee S. Precipitation of the δ-Ni3Nb phase in two nickel base superalloys. Metall Trans A. 1988;19:453–465. doi:10.1007/BF02649259.

[8] Lass EA, Stoudt MR, Williams ME, et al. Formation of the Ni3Nb δ-phase in stress-relieved Inconel 625 produced via laser powder-bed fusion additive manufacturing. Metall Mater Trans A. 2017;48:5547–5558. doi:10.1007/s11661-017-4304-6.

[9] Hassan B, Corney J. Grain boundary precipitation in Inconel 718 and ATI 718Plus. Mater Sci Technol. 2017;33:1879–1889. doi:10.1080/02670836.2017.1333222.

[10] Stoudt MR, Lass EA, Ng DS, et al. The influence of annealing temperature and time on the formation of δ-phase in additively-manufactured Inconel 625. Metall Mater Trans A. 2018;49:3028–3037. doi:10.1007/s11661-018-4643-y.

[11] Cortial F, Corrieu JM, Vernot-Loier C. Influence of heat treatments on microstructure, mechanical properties, and corrosion resistance of weld alloy 625. Metall Mater Trans A. 1995;26:1273–1286. doi:10.1007/BF02670621.

[12] Xu F, Lv Y, Liu Y, et al. Effect of heat treatment on microstructure and mechanical properties of Inconel 625 alloy fabricated by pulsed plasma Arc deposition. Phys Procedia. 2013;50:48–54. doi:10.1016/j.phpro.2013.11.010.

[13] Andersson J-O, Helander T, Höglund L, et al. Thermo-Calc & DICTRA, computational tools for materials science. Calphad. 2002;26:273–312. doi:10.1016/S0364-5916(02)00037-8.

[14] Li S, Wei Q, Shi Y, et al. Microstructure characteristics of Inconel 625 superalloy manufactured by selective laser melting. J Mater Sci Technol. 2015;31:946–952. doi:10.1016/j.jmst.2014.09.020.

[15] Hönnige J, Seow CE, Ganguly S, et al. Study of residual stress and microstructural evolution in as-deposited and inter-pass rolled wire plus arc additively manufactured Inconel 718 alloy after ageing treatment. Mater Sci Eng A. 2021;801:140368. doi:10.1016/j.msea.2020.140368.

[16] Xing X, Di X, Wang B. The effect of post-weld heat treatment temperature on the microstructure of Inconel 625 deposited metal. J Alloys Compd. 2014;593:110–116. doi:10.1016/j.jallcom.2013.12.224.

[17] Lindwall G, Campbell CE, Lass EA, et al. Simulation of TTT curves for additively manufactured Inconel 625. Metall Mater Trans A. 2019;50:457–467. doi:10.1007/s11661-018-4959-7.

[18] Keller T, Lindwall G, Ghosh S, et al. Application of finite element, phase-field, and CALPHAD-based methods to additive manufacturing of Ni-based superalloys. Acta Mater. 2017;139:244–253. doi:10.1016/j.actamat.2017.05.003.

[19] Rodrigues TA, Escobar JD, Shen J, et al. Effect of heat treatments on 316 stainless steel parts fabricated by wire and arc additive manufacturing: microstructure and synchrotron X-ray diffraction analysis. Addit Manuf. 2021;48:102428. doi:10.1016/j.addma.2021.102428.